International Journal of Heat and Technology
Vol. 36, No. 2, June, 2018, pp. 741-751
Journal homepage: http://iieta.org/Journals/IJHT

Performance evaluation of solar air heater equipped with louvered fins

Subhash Chand*, Prabha Chand

Department of Mechanical Engineering, National Institute of Technology, Jamshedpur, Jharkhand 831014, India

Corresponding Author Email: subhash.citm@gmail.com

https://doi.org/10.18280/ijht.360241

Received: 26 December 2017
Accepted: 20 April 2018

Keywords:
effective efficiency 1, solar air heater 2, louvered fin 3, thermal efficiency 4

ABSTRACT

The current work deals with the thermal performance of louvered finned solar air collector. The study involves evaluating various parameters such as temperature rise, thermal efficiency, effective efficiency and insolation compared to that of plane solar air heater. It is observed that at minimum duct height and minimum fin spacing the thermal efficiency shows a noticeable enhancement but the effective efficiency reduced at higher mass flow rate, even may be less than plane solar air heater. This is because of higher pressure drop that occurs at higher mass flow rate. Further the result revealed that the increasing solar intensity leads to increase in temperature rise linearly while the solar intensity has a little effect on thermal efficiency for a given mass flow rate.

1. INTRODUCTION

The solar air heater has a vital place in solar thermal system. The most obvious and effective approach use the solar energy is conversion it in to thermal energy particularly for heating application. Because of its inherent simplicity solar air heater has low operating cost and is widely used in various commercial applications such as crop drying , space heating and industrial and agricultural drying etc. The size, shape, material and layout of collector are factors influencing the thermal performance of solar air heater. Several researchers have undertaken in-depth studies account for the performance of the solar collectors by connecting fins, fins with baffles, fins with perforation, pin fin, artificial roughness, packed bed etc.

To glance upon the work in past decades involving, particularly the studies of absorber surfaces. In this context, Yeh and Ho [1] analyzed the external recycle effect on the performance characteristics of flat plate solar air heater with internal fins. On the other hand, effect of internal recycle was examined by Yeh [2]. The result revealed that about more than 100% in thermal efficiency is obtained by recycling operation particularly at higher inlet air temperature with lower flow rate. Karim and Hawlader [3] analyzed the v-corrugated and flat plate finned solar collector both theoretically and experimentally over an extensive range of operating and different designs conditions. The study demonstrate that the v-corrugated collector efficiency was more as compared to the plane solar collector. For double pass operation, thermal efficiency was improved for all three types of collector whereas the improvement in the thermal efficiency was high in the simple solar collector as compared to the v-corrugated collector. Handoyo and Ichsani [4] investigated the v-corrugated duct with delta shaped obstacles. They showed that enhanced the friction factor and Nusselt number by 19.9 times and 3.46 times respectively and can be obtained by placing the obstacles on the collector with small spacing, and also concluded that the height of delta shaped obstacles was equal to its optimal spacing ratio. Chabane et al. [5] performed a study the thermal performance and heat transfer of single pass solar air heater experimentally with five longitudinal fins which are attached to the absorber and found substantial enhancement in thermal efficiency. Sabzpooshani et al. [6] analyzed the performance of single pass solar air heater with attached of fins and baffles. They observed that increasing the numbers of fines as well as baffles width and reducing the distance between baffles are efficient at lower mass flow rate, whereas reverse trend is observed at higher mass flow rates. Priyam and Chand [7] developed mathematical model to study the thermohydraulic and thermal performance of wavy finned absorber solar air heater and evaluated the effect of fin spacing and mass flow rate. Ho et al. [8] carried out an experimental study and analytical study of the double pass solar air heaters with recycled baffled attached with fins. They investigated the effects of recycled ratio and mass flow rate on the power consumption and heat collection. Further, Maheshwari et al. [9] carried out a study of heat transfer and thermal efficiency in such an absorber plate with half perforated baffles. A significant improvement in thermal efficiency was obtained in an experimental study carried out on solar air heater having absorber plate with half perforated baffles.

In many studies [10-15] experimental and theoretical study on louvered fins were tested in the heat exchanger. In the corrugated louvered fin heat exchangers studied by Shah and Sakulic [16]. Another study by Kraus [17] was on flat tube corrugate louvered fin. Webb and Trauger [10] analyzed the flow pattern in the louvered finned heat exchanger. The geometrical parameters such as fin pitch, louvered angle and louvered pitch were varied to study their influence on the flow pattern. Sahnoun and Webb [11] investigated the prediction of friction factor and heat transfer for the louver finned geometry. Their model was based on the channel flow efficiency and boundary layer. This model was flexible enough to encompass independent specifications of all the major geometric parameters of the louvered fin.

The literatures has substantial amount of work on solar air heater with different types of fins likes triangular fins, longitudinal fins, wavy fins etc. Also, the use of these fins certainly better thermal performance the plain solar air heater.

Despite of this, a detailed workout on louvered fin based on solar air heater is yet to appear in the literature. In light of this knowledge, the author are motivated to performance analysis on louvered finned based solar air heater to manifest the grade of thermal and thermohydraulic performance it has to offer. The advantage of employing louvered fins is that it keeps the air flow normal to its louvers, thereby increasing the surface area and hence enhancing the rate of heat transfer. The added advantage to this is the associated turbulent mixing of air flow which impedes the growth of thermal boundary layer from the leading edge.

The present work, involves an analytical study of louvered fin solar air heater with an objective of evaluating its thermal as well as thermohydraulic performance. The parameters considered for this purpose are geometry of louvered fin, fin spacing and mass flow rate on thermohydraulic and thermal performance has been investigated. Further, the results are compared with that of plane solar air heater.

2. THERMAL ANALYSIS

The louvered finned solar air heater considered in this work has a single pass between the bottom plate and absorber plate. Heat transfer coefficients and all geometrical parameter for the louvered fin associated with system as shown in Fig.1 and Fig.2. Following assumptions has been considered for simplifying the analysis.

i. The flow is Steady.
ii. The air heater is leak proof.
iii. Temperature drop is negligible through the absorber plate and the glass cover.
iv. Thermal conductivity is constant throughout the flow channel.

2.1. Energy balance equations

Consider L2 be the width of the collector and dx be the thickness at a distance x from the inlet section as shown in Fig. 1. Fig.2 shows the geometrical description of fins and Fig.3 shows the behavior of flow through the louvered fins. For the different component of solar air heater energy balance equation can be written as.

For absorber plate:

$$I\alpha_1\tau_c = U_t(T_1 - T_a) + h_{c,1f}\left(T_1 - T_f\right) + h_{r,12}\left(T_1 - T_2\right) + h_{ff}\phi_{fin}(T_1 - T_f) \quad (1)$$

For bottom plate

$$h_{r,12}\left(T_1 - T_2\right) + h_{c,f2}\left(T_f - T_2\right) = U_b\left(T_2 - T_a\right) \quad (2)$$

For air stream

$$\frac{\dot{m}C_p}{L_2}\frac{dT}{dx} = h_{c,1f}\left(T_1 - T_f\right) + h_{ff}\phi_{fin}(T_1 - T_f) + h_{c,2f}\left(T_2 - T_f\right) \quad (3)$$

In above equations, I (W/m^2) is the solar intensity, α_1 and T_1 (K) the absorptivity and plate temperature of the absorber plate respectively, T_f (K) and T_2 (K) are the fluid temperature and bottom plate temperature respectively, C_p is the specific heat of fluid, the convective heat transfer between the air stream and absorber plate ($h_{c,1f}$) and the air stream and bottom plate ($h_{c,f2}$),

The effectiveness of fin ϕ_{fin} is defined as,

$$\phi_{fin} = 1 + \left(\frac{A_f}{A_c}\right)\eta_f \quad (5)$$

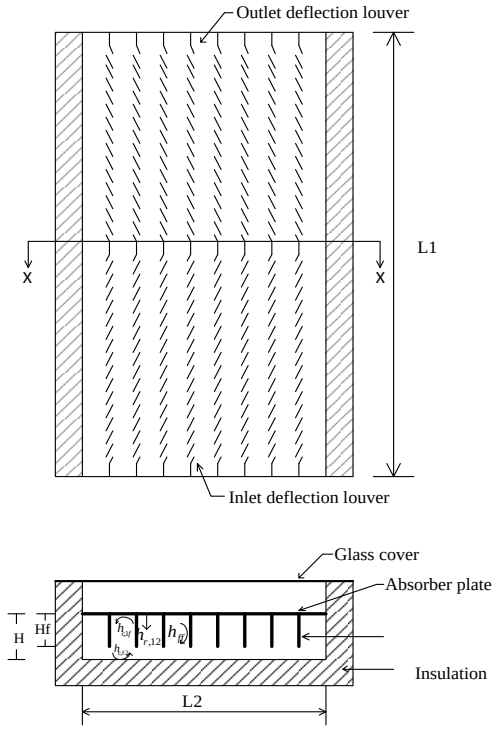

Figure 1. Physical model of solar air heater with louvered fins

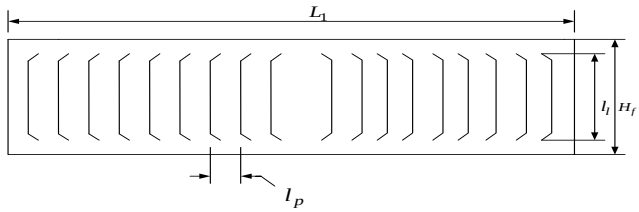

Figure 2. Geometrical description of louvered fin

Total surface area of fin and fin efficiency is calculated as,

$$A_f = \left(2H_f L_1 + 2H_f t + \left(2l_p t + l_l t\right)N_l + L_1 t\right)n \quad (6)$$

$$A_c = L_2 L_1 - ntL_1 \quad (7)$$

$$\eta_f = \frac{\tanh\left(mH_f\right)}{mH_f} \quad (8)$$

where $m = \sqrt{\frac{2h_{c,ff}}{k_{fin}t}}$

Solving the energy balance equation (1) and equation (2) for getting the temperature difference $\left(T_1 - T_f\right)$ and $\left(T_2 - T_f\right)$.

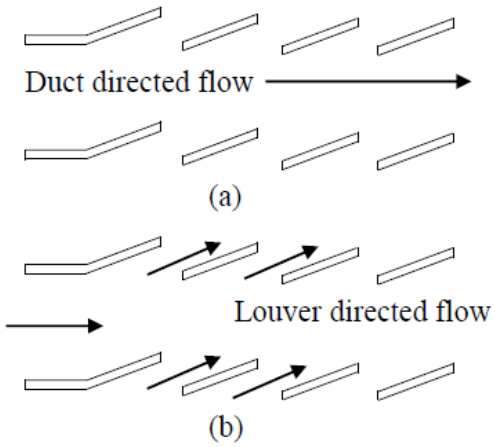

Figure 3. (a) Duct directed flow and (b) Louvered directed flow through a louvered channel

$$T_1 - T_f = \frac{\left[I\alpha_1\tau_c\left(h_{r,12}+h_{c,ff}+U_b\right)-\left(U_t h_{r,12}+U_t h_{c,ff}+U_t U_b+h_{r,12}U_b\right)\left(T_f-T_a\right)\right]}{\left[\left(U_t+h_{c,1f}+h_{r,12}+h_{c,ff}\phi_{fin}\right)\left(h_{r,12}+h_{c,ff}+U_b\right)-\left(h_{r,12}\right)^2\right]} \quad (9)$$

$$T_2 - T_f = \frac{\left[h_{r,12}I\alpha_1\tau_c-\left(h_{r,12}U_t+U_tU_b+h_{c,1f}U_b+h_{r,12}U_b+h_{c,ff}\phi_{fin}U_b\right)\left(T_f-T_a\right)\right]}{\left(\left(U_t+h_{c,1f}+h_{r,12}+h_{c,ff}\phi_{fin}\right)\left(h_{r,12}+h_{c,ff}+U_b\right)-\left(h_{r,12}\right)^2\right)} \quad (10)$$

Substituting the value of $\left(T_1 - T_f\right), \left(T_2 - T_f\right)$ in equation (3), and obtain

$$\frac{dT}{dx} = \frac{L_2 F}{\dot{m}Cp}\left(I\alpha_1\tau_c - U_L\left(T_f - T_a\right)\right) \quad (11)$$

where

$$F = \frac{\left(h_{c,1f}+h_{ff}\phi_{fin}\right)\left(h_{r,12}+h_{c,1f}+U_b\right)+h_{c,1f}h_{r,12}}{\left(\left(U_t+h_{c,ff}+h_{r,12}+h_{ff}\phi_{fin}\right)\left(h_{r,12}+h_{ff}+U_b\right)-\left(h_{r,12}\right)^2\right)} \quad (12)$$

$$U_L = U_t + \frac{h_{r,12}U_b}{h_{r,12}+h_{c,ff}+U_b} + \frac{1}{F}\left(\frac{h_{c,1f}U_b}{h_{r,12}+h_{c,1f}+U_b}\right) \quad (13)$$

F and U_L are the collector efficiency factor and total heat loss coefficient respectively. Integrating the equation (11) and substituting the boundary conditions $x = 0, T_f = T_{fi}$ we obtain the temperature distribution

$$\frac{\left(\frac{I\alpha_1\tau_c}{U_L}+T_a\right)-T_f}{\left(\frac{I\alpha_1\tau_c}{U_L}+T_a\right)-T_{fi}} = \exp\left[-\frac{L_2 F U_L x}{\dot{m}C_p}\right] \quad (14)$$

The fluid outlet temperature T_{fo} (K) is obtained $T_f = T_{fo}, x = L_1$

$$\frac{T_{fo}-T_{fi}}{\left(\frac{I\alpha_1\tau_c}{U_L}+T_a\right)-T_{fi}} = 1-\exp\left[-\frac{L_2 F U_L L_1}{\dot{m}C_p}\right] \quad (15)$$

Useful heat gain rate for the collector.

$$Q_u = \dot{m}C_p\left(T_{fo}-T_i\right) \quad (16)$$

$$Q_u = \frac{\dot{m}C_p}{U_L}\left(I\alpha_1\tau_c - U_L\left(T_{fi}-T_a\right)\right)\left\{1-\exp\left[-\frac{FU_L A_p}{\dot{m}C_p}\right]\right\} \quad (17)$$

$$Q_u = F_r A_p\left(I\alpha_1\tau_c - U_L\left(T_{fi}-T_a\right)\right) \quad (18)$$

where, F_r is the heat removal factor.

$$F_r = \frac{\dot{m}C_p}{U_L A_p}\left\{1-\exp\left[-\frac{FU_L A_p}{\dot{m}C_p}\right]\right\} \quad (19)$$

2.2. Heat transfer coefficient and pressure drop

An empirical equation for the top loss coefficient $\left(U_t\right)$ was given by Duffie and Beckman[18]

$$U_t = \left[\frac{M}{\left(\frac{C}{T_1}\right)\left(\frac{T_1-T_a}{M+f}\right)^{0.252}}+\frac{1}{h_w}\right]^{-1} + \left[\frac{\sigma\left(T_1^2+T_a^2\right)\left(T_1+T_a\right)}{\frac{1}{\varepsilon_p+0.0425M\left(1-\varepsilon_p\right)}+\frac{2M+f-1}{\varepsilon_c}-M}\right] \quad (20)$$

where,

$$f = \left(\frac{9}{h_w}-\frac{30}{h_w^2}\right)\left(\frac{T_a}{316.9}\right)\left(1+0.091M\right)$$

$$C = 204.429\left(\cos\beta\right)^{0.252}/\mathrm{w}^{0.24}$$

where the bottom loss coefficient is,

$$U_b = \frac{K_{ins}}{t_{ins}} \quad (21)$$

The convective heat transfer coefficients between the atmospheric air and glass cover can be given by the relation Watmuff et al. [19]

$$h_w = 2.8 + 3.0V_w \tag{22}$$

The radiation heat transfer coefficient between the absorber plate and bottom plate is calculated as,

$$h_{r,12} = \frac{\sigma\left(T_1^2 + T_2^2\right)\left(T_1 - T_2\right)}{\frac{1}{\varepsilon_1} + \frac{1}{\varepsilon_2} - 1} \tag{23}$$

Heaton et al. [20] presented the convective heat transfer coefficient for laminar flow between the rectangular channel,

$$Nu_{12} = 4.4 + \frac{0.00398\left(\frac{0.7\,\mathrm{Re}\,D_h}{L_1}\right)^{1.66}}{1 + 0.00114\left(\frac{0.7\,\mathrm{Re}\,D_h}{L_1}\right)^{1.12}} \tag{24}$$

For turbulent flow in rectangular channel heat transfer coefficient correlation is presented by Keys [21],

$$Nu_{12} = 0.00158\,\mathrm{Re}^{0.8} \tag{25}$$

Nusselt number is calculated for louvered finned solar air heater using the correlation in terms of Colburn factor (j) Dong et al. [22],

$$j = 0.26712\left(\mathrm{Re}_{lp}\right)^{-0.1944}\left(\frac{\theta_l}{90}\right)^{0.257}\left(\frac{w}{l_p}\right)^{-0.5177}\left(\frac{H_f}{l_p}\right)^{-1.9045}\left(\frac{l_l}{l_p}\right)^{1.7159}\left(\frac{L_1}{l_p}\right)^{-0.2147}\left(\frac{t}{l_p}\right)^{-0.05} \tag{26}$$

where, θ_l is the louvered angle, l_p (m) is the louvered pitch, l_l (m) is the louvered length, Re_{lp} is the louvered Reynolds number, t (m) is the thickness of fin.

$$Nu_{12} = j\,\mathrm{Re}\,\mathrm{Pr}^{0.4} \tag{27}$$

Convective heat transfer coefficient,

$$h_{c,1f} = h_{c,2f} = h_{c,ff} = \frac{Nu_{12}k_{air}}{D_h} \tag{28}$$

The hydraulic diameter (D_h) is given by,

$$D_h = \frac{4\left(wH - t\left(H_f - t\right)\right)L_1}{2L_1\left(w - t\right) + \left(2L_1H_f - t\right)} \tag{29}$$

Reynolds number of the flow channel is given by,

$$\mathrm{Re} = \frac{\rho V D_h}{\mu} \tag{30}$$

where Reynolds number between the louver pitch (Re_{lp}) and Reynolds number on the louver (Re_L) are given by Webb and Trauger [10]

$$\mathrm{Re}_{lp} = \frac{V_l \times l_p}{\upsilon} \tag{31}$$

$$\mathrm{Re}_L = \frac{V \times l_p}{\upsilon} \tag{32}$$

Following empirical correlation is developed by Web and Trauger [10] to find the critical Reynolds number.

$$\mathrm{Re}_{l_1} = 828\left(\frac{\theta_l}{90}\right)^{-0.34} \tag{33}$$

An appropriate air velocity over the louvers (V_l) is require to calculate the Reynolds number in equation (31). Factors affecting the louvers' velocity are (i) the acceleration of the flow due to the angular redirection caused by the louvers, (ii) the flow efficiency.

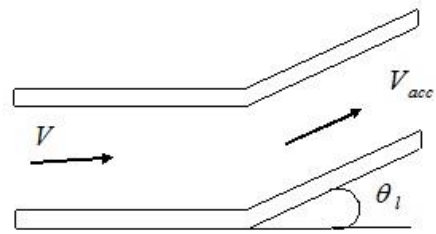

Figure 4. Flow acceleration caused by louvered angle

Fig. 4 shows that the flow speed increase from V to V_{acc}, because of reduced the flow area.

$$V_{acc} = V\left(\frac{w - t}{w\cos\theta_l - t}\right) \tag{34}$$

Separate flow efficiency correlation is required to find the Reynolds number. The following correlation given by Webb and Trauger [10] predicts the flow efficiency.

For $\mathrm{Re}_l > \mathrm{Re}_{l_1}$

$$Fe_L = 0.95\left(\frac{l_p}{w}\right)^{0.23} \tag{35}$$

When $\mathrm{Re}_l < \mathrm{Re}_{l_1}$

$$Fe = 0.091\left(\mathrm{Re}_l\right)^{0.39}\left(\frac{l_p}{w}\right)^{0.44}\left(\frac{\theta_l}{90}\right)^{0.3} \tag{36}$$

The relationship between (V_l) and (V_{acc}) is given by,

$$V_l = V_{acc} \times Fe \tag{37}$$

The pressure drop (Δp) of air in the rectangular channel attached with louvered fins is given by,

$$\Delta p = \frac{4 f \rho L_1 V^2}{2 D_h} \tag{38}$$

where, f is the fanning friction factor calculated from the correlation developed by Dong et al. [22].

$$f = 0.54486\left(\mathrm{Re}_{lp}\right)^{-0.3068}\left(\frac{\theta_l}{90}\right)^{0.444}\left(\frac{w}{l_p}\right)^{-0.9925} \left(\frac{H_f}{l_p}\right)^{0.5458}\left(\frac{l_l}{l_p}\right)^{-0.2003}\left(\frac{L_1}{l_p}\right)^{0.0688} \tag{39}$$

The air temperature is in the range of 280-450K. The correlation used to calculate the density, viscosity and thermal conductivity respectively.

$$\rho = 3.9147 - 0.016082 T_f + 2.9013\times10^{-5} T_f^2 - 1.9407\times10^{-8} T_f^3 \tag{40}$$

$$\mu = \left(1.6157 + 0.06523 T_f - 3.0297\times10^{-5} T_f^2\right)\times10^{-6} \tag{41}$$

$$k = \left(0.0015215 + 0.097457 T_f - 3.3322\times10^{-5} T_f^2\right)\times10^{-3} \tag{42}$$

2.3. Thermal and thermohydraulic performance

Thermal efficiency of a solar collector is define as;

$$\eta = \frac{Q_u}{I \times A_c} \tag{43}$$

The thermohydraulic performance of solar collector and effective efficiency are defined as;

$$\eta_{eff} = \frac{Qu - \frac{P_{mech}}{C_f}}{I \times A_c} \tag{44}$$

where, C_f is the conversion factor which accounts for various efficiencies, and its value is taken as 0.18.

To overcome the pressure loss in the flow channel the mechanical power (P_{mech}) is required and can be evaluate by:

$$P_{mech} = \frac{\dot{m}\,\Delta p}{\rho} \tag{45}$$

3. CALCULATION PROCEDURE

A computer code was developed by considering the following system, operating condition and system properties as listed in given below. The iteration process is described as follows.

1. Initial value of T_1, T_2, T_f are assumed.
2. Heat transfer coefficients is calculated using equations (23) and (28).
3. The new value of T_1, T_2, T_f is calculated
4. If the absolute error of calculated temperature is within the tolerance of 10^{-4} with respect to old value, the process is ended otherwise replace the old value with new ones and repeat the iteration from step 2
5. After converse is achieved the value of mean temperature is found out and after using the above results the thermal and thermohydraulic efficiency is calculated using equation (43) and (44)

A Flow chart represent the calculation procedure in figure 5.

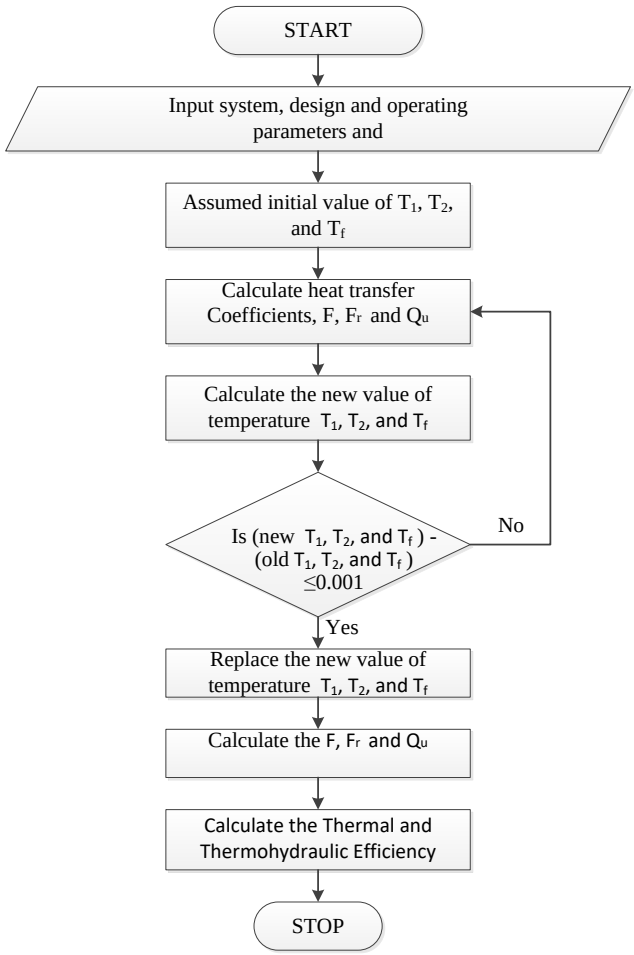

Figure 5. Flow chart of calculation procedure

4. VALIDATION OF MATHEMATICAL MODEL

Results of Karwa et al. 23] have been used for validation purpose to show variations in thermal efficiency of louvered finned and plane solar air heater by maintaining all the parameters as shown in Figure 6. The mean deviation ±5.3% from the experimental values of thermal efficiency of plane solar air heater is given by Karwa et al. [23]. When mass flow rate increases from 0.008kg/s to 0.035kg/s, an average enhancement of 21.25% is obtained in the thermal efficiency of louvered finned solar air heater. This results reveals a good accord between the mathematical and theoretical values, which confirm the correctness of results obtained in the present theoretical model.

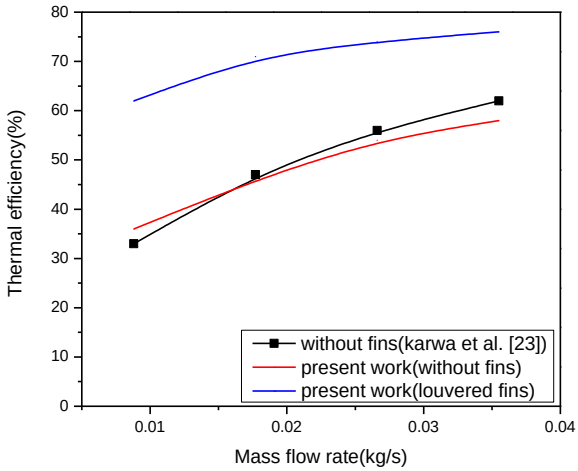

Figure 6. Comparison of thermal efficiency of present work with Karwa et al. [23]

5. RESULTS AND DISCUSSION

In this section the performance of solar air heater equipped with the louvered fin for varying mass flow rate, fin spacing, fin height, duct height and louvered fin geometry is discussed. The results have been compared with that of the simple solar air heater. For the sake of numerical calculation following design and fixed parameters are considered:

$L_1 = 1.2$ m , $I = 950$ W/m^2 , $L_2 = 0.6$ m , $H = 0.02$ m $- 0.05$ m , $H_f = 0.018 - 0.048$ m , $t = 0.0025$ m , $l_p = 0.015$ m , $l_l = 0.014$ m, 0.024 m , $\theta_l = 20^o$, $V_w = 2.5$ m/s , $K_f = 50$ W/mK , $T_a = 300$ K , $T_i = 303$ K , , $\alpha_c = 0.11$, $\varepsilon_1 = 0.95$, $\varepsilon_2 = 0.95$, $\varepsilon_c = 0.90$, $\alpha_1 = 0.96$. For fin spacing $w = 1$ cm, 2.5 cm, 5 cm. and mass flow range of $\dot{m} = 0.0083$kg/s $- 0.083$kg/s .

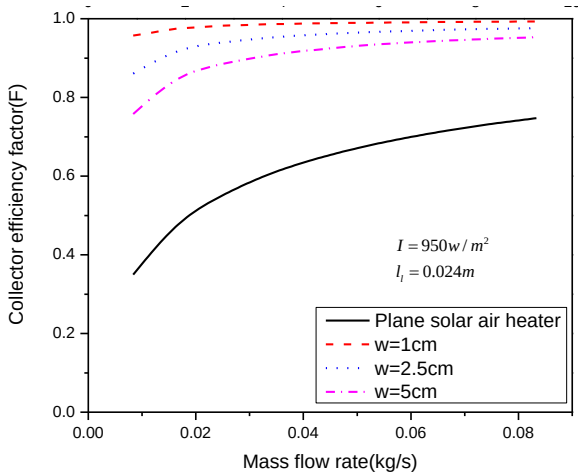

Figure 7. Collector efficiency factor versus mass flow rate

5.1. Effects of fin spacing

Figure 7 depicts the influence of mass flow rate on collector efficiency factor for different values of louvered fin spacing and plane solar air heater. The value of collector efficiency factor rises with the mass flow rate for all values of fin spacing and plane solar air heater. The results revealed that the collector efficiency factor increases with decreasing fin spacing at constant mass flow rate. This is because collector efficiency factor is a function of heat transfer coefficients, the fin spacing decreases as the effective heat transfer area increases.

Figure 8 shows the effect of mass flow rate for different fin spacing on heat removal factor and that for simple solar air heater. Result shows that for all range of mass flow rate and all values of fin spacing the heat removal factor increases. It can be noticed that the heat removal factor increases with decreasing values of fin spacing at a constant mass flow rate. The reason for this is that the decrease in temperature rise through the collector and corresponding increase in the useful energy gain. This increases may be the cause of that increase in the value of heat removal factor.

The variation in total loss coefficient for various fin spacing and plane solar air heater with respect to mass flow rate has been plotted in the Figure 9. The total heat loss coefficient of the louvered fin drops with increasing the mass flow rate for all values of fin spacing's. It has been found that the total loss coefficient increased with increasing the fin spacing. This is due to the fact that as fin spacing increases, the surface area of heat transfer decreases and along with it the mean plate temperature decreases which holds true for all mass flow rate. This will lead to increase in the total loss coefficient.

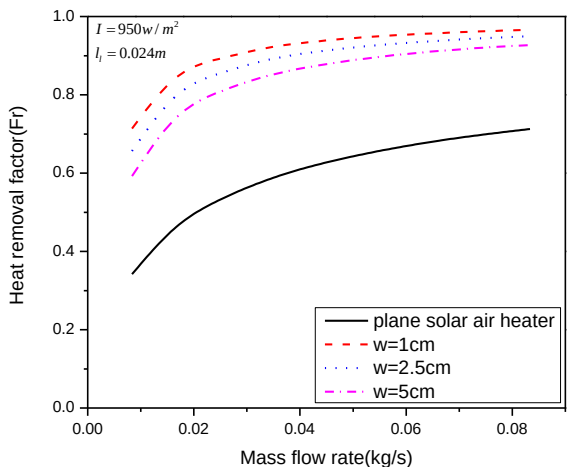

Figure 8. Heat removal factor versus mass flow rate

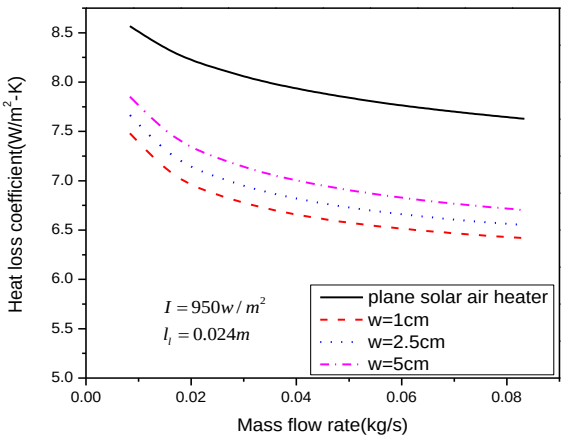

Figure 9. Variation of total heat loss coefficient varies with mass flow rate

Figure 10 and figure 11 shows the variation of temperature rise and thermal efficiency curves for various louvered fin

spacing plotted against mass flow rate and compared with plane solar air heater. It is apparent from the figure that the trend of variation in temperature rise and thermal efficiency is reversed with increasing values of mass flow rate, thermal efficiency increases whereas temperature rise decreases with the given range of mass flow rate. It is also seen that the thermal efficiency and temperature rise is increased with decreasing fin spacing at constant mass flow rate. This can be attributed to decreases in the temperature rise which causes significant rise in the useful energy gain and heat transfer surface area.

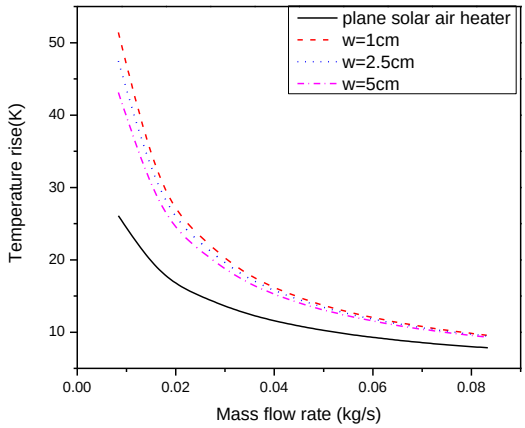

Figure 10. Temperature rise versus mass flow rate for different fin spacing

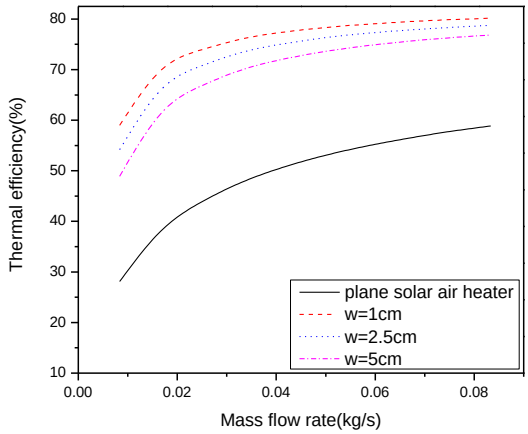

Figure 11. Thermal efficiency versus mass flow rate for different fin spacing

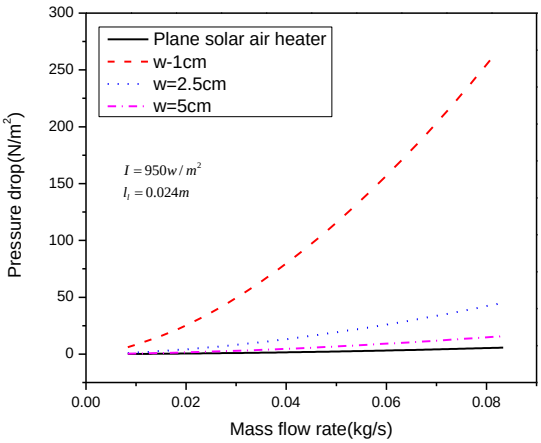

Figure 12. Pressure drop versus mass flow rate for different fin spacing

Figure 12 shows the effect of mass flow rate on pressure drop across the collectors for different louvered fins spacing and plane solar air heater. Increasing the mass flow rate causes the pressure drop to increase as shown in fig. It can be observed that for minimum fin spacing pressure drop goes up maximum. This may be due to fact that at lower fin spacing, randomness of fluid particle increases due to increase in fluid velocity which in turn increases the friction losses. Therefore, high power required to overcome these losses.

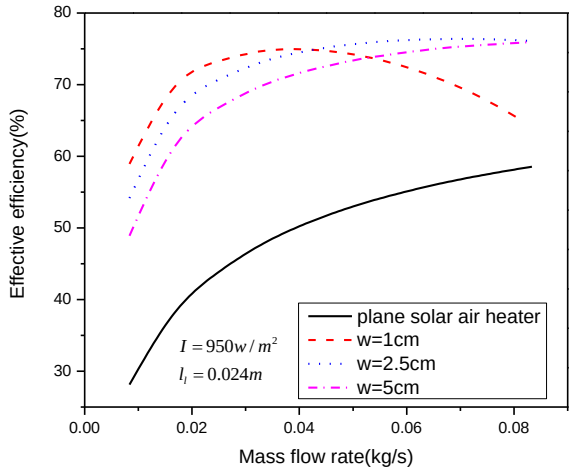

Figure 13. Effective efficiency versus mass flow rate for different fin spacing

Figure 13 illustrate the variation of effective efficiency for various louvered fins spacing with respect to mass flow rate and it is compared with that of plane solar air heater. The effective efficiency is termed as the efficiency which accounts for the hydraulic flow in thermal fluid. It is evident from the figure that the effective efficiency firstly increases with mass flow rate, attains a maximum value and then starts dropping with further increase in the value of mass flow rate. It can be observed that the effect of pressure drop is insignificant with increase in mass flow rate up to maximum effective efficiency point. Also, the effective efficiency starts dropping with further increase in mass flow rate because high equivalent thermal energy needed for producing the work energy which is required to do down the losses in pressure energy.

5.2. Effects of fin height and duct height

Figure 14 shows the effect of different fin height to collector efficiency factor at various mass flow rate for constant fin spacing (w=1cm). It can be noticed from the figure that the collector efficiency factor increases for all fin height with increasing mass flow rate. It is also observed that increase in height of louvered fin along with increase in duct height, which in turn decreases the collector efficiency factor. This is because of the increased surface area of louvered fins. However it also causes a considerably drop in the convective heat transfer coefficient.

The effect of mass flow rate on the heat removal factor for constant fin spacing (w=1cm) at different fin height have been plotted in Figure 15. The results reveal that the heat removal factor increases with increase in mass flow rate for all fins height. It can be observed that the increase in louvered fin height decreases the heat removal factor for all mass flow rate. This is because the increase in values of fin height decreases the surface conductance of fins.

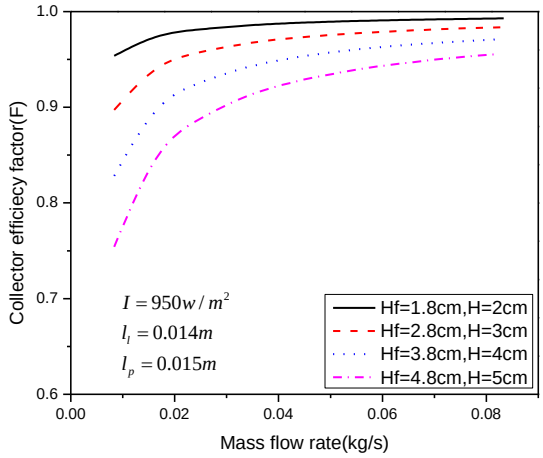

Figure 14. Variation of collector efficiency factor with mass flow rate

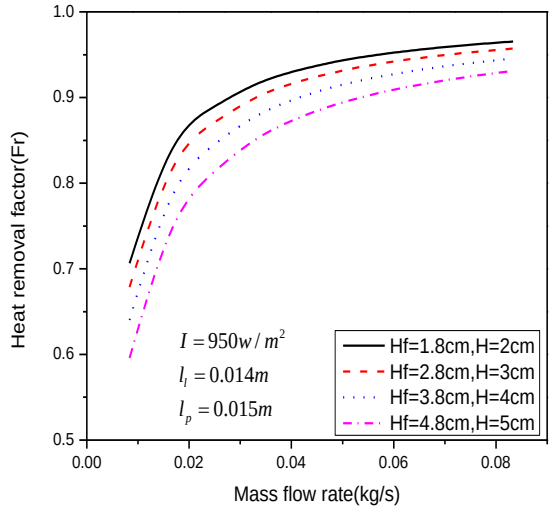

Figure 15. Heat removal factor versus mass flow rate

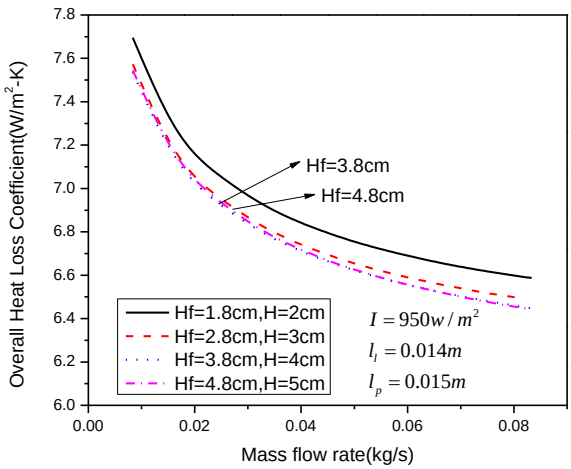

Figure 16. Variation of total heat loss coefficient with mass flow rate

Figure 16 shows the effect of different fin height to total loss coefficient at various mass flow rate for constant fin spacing (w=1cm). From the plots it is observed that the total heat loss coefficient keeps on decreasing when fin height changes from1.8cm to 3.8cm after which the total heat loss coefficient is seen to increase. The minimum value of total heat loss coefficient is observed at Hf = 3.8cm which is the optimum.

Figure 17 and figure 18 illustrates the changes in the thermal efficiency and temperature rise with mass flow rate at constant fin spacing for different fin height. It is evident from the figure that the trend of variation of temperature rise and thermal efficiency are reversed with mass flow rate, thermal efficiency increases whereas temperature rise drops with mass flow rate. It is also observed that the thermal efficiency and temperature rise decreases for higher value of fin height (Hf =4.8cm). This may be due to the increase the fin height which causes decreases in the surface conductance of fins.

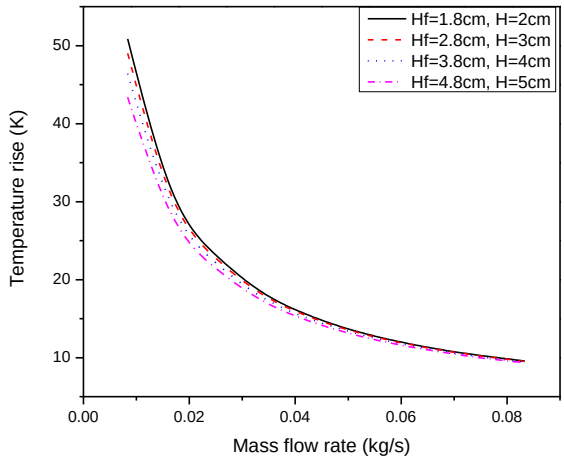

Figure 17. Temperature rise versus mass flow rate for different fin height

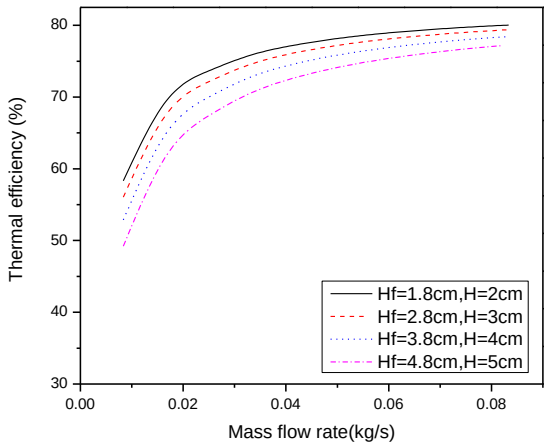

Figure 18. Thermal efficiency versus mass flow rate for different fin height

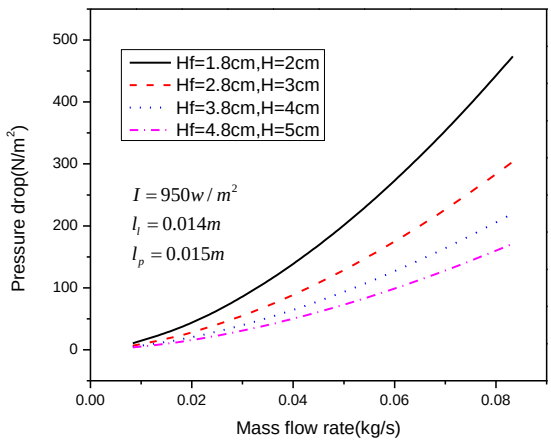

Figure 19. Pressure drop versus mass flow rate for different fin height

Figure 19 depicts the effect of fin height on pressure drop for various mass flow rate throughout the collector. From the figure it is evident that the pressure drops increases with decreases in fin height. This may due to fact that decrease the fin height increases the velocity of air flowing through the channel which leads to increase the randomness of fluid particle consequently increases the friction losses.

Figure 20 illustrate the influence of mass flow rate on effective efficiency of louvered fin solar air heater for various fin height at constant fin spacing w=1cm. It is noticed from the fig. that the effective efficiency first increases up to mass flow rate (m= 0.041kg/s), attains a maximum value and then drops with further rise in mass flow rate. It is also seen that for minimum fin height (Hf = 1.8cm) the effective efficiency decreases pre-eminent beyond mass flow rate of 0.033kg/s onwards. This due to fact that the pressure drop is more for lower value of fin height.

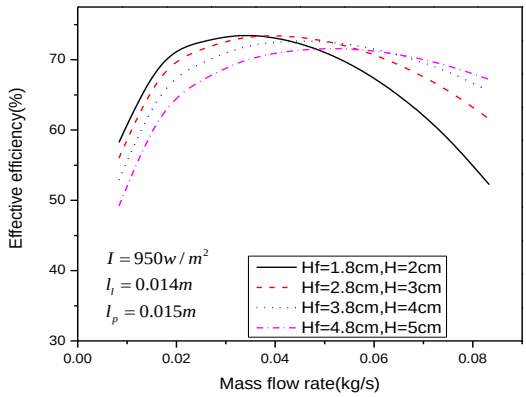

Figure 20. Effective efficiency versus mass flow rate for different fin height

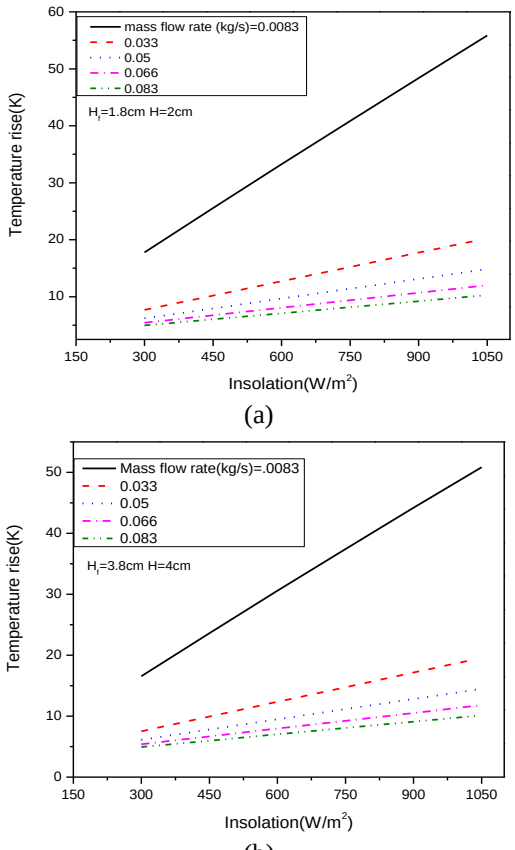

Figure 21. Temperature rise versus insolation for different mass flow rate

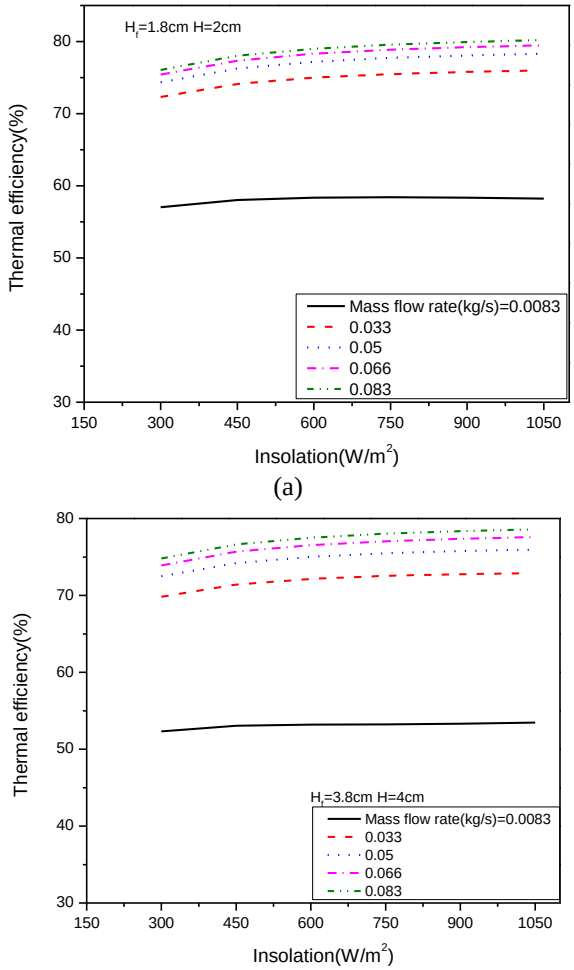

Figure 22. Thermal efficiency versus insolation for different mass flow rate

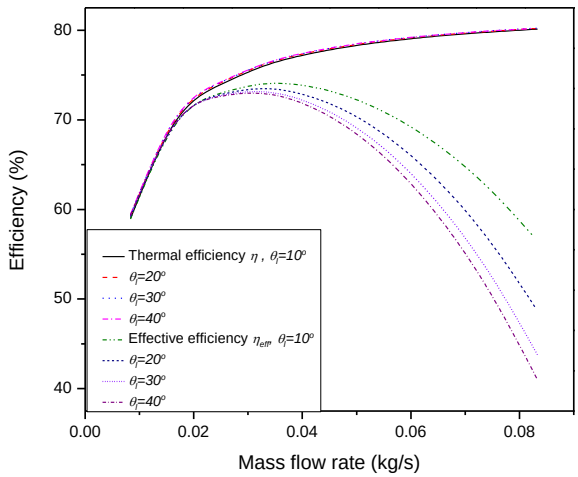

Figure 23. Thermal efficnecy and effective efficiency versus mass flow flow rate with diffrent louvered angles

Figure 21 (a) and 21(b) shows the effect of isolation on the temperature rise for different mass flow rate at fin height 1.8cm and 3.8cm for constant spacing 1cm. The temperature rise increases linearly with increase in isolation at all values of mass flow rate. From the results shows that the temperature rise decreases with increases in mass flow rate.

The influence of solar intensity on thermal efficiency for fin height 1.8cm and 3.8cm at constant fin spacing have been plotted in figure 22(a) and 22(b) respectively. It is evident that the variation of solar intensity has little effect on thermal efficiency for each value of mass flow rate. This is due to fact the isolation has no significant influence on convection heat transfer between the fins and fluids.

Figure 23 illustrates the influence of mass flow rate on thermal efficiency and effective efficiency of louvered fin solar air heater at constant fin spacing w=1cm and different louvered angle. It is noticed from the figure that the thermal efficiency increases with increasing mass flow rate, but the effective efficiency first increases up to mass flow rate (m= 0.041kg/s), attains a maximum value and then drops with further rise in mass flow rate. It is also seen that for increase in values of the louvered angle, enhancement in thermal efficiency is very low, while the effective efficiency drops significantly. This is due to fact the increasing the louvered angle, increases the compactness of absorber plate which in turn increases the pressure drop thus leading to decrease in effective efficiency.

6. CONCLUSIONS

The current work is aimed to analyze a thermohydraulic and thermal performance of louvered finned solar air heater. This analytical study is compared with a simple solar air heater. Louvered finned solar air heater increases heat transfer rate due to the flow is louvered directed. Factors on which the efficiency of solar air heater depends are: surface geometry and mass flow rate of the collector.

The value of total heat loss coefficient, heat removal factor, collector efficiency factor, and thermal efficiency has been obtained from the energy balance equation for louvered finned solar air heater. The results have revealed that the louvered finned solar air heater with constant fin spacing (w = 1cm) and fin height Hf = 2.8cm yields a higher value of thermal efficiency as compared to that of plane solar air heater. For fin spacing 5cm to 1 cm, the thermal efficiency increases from 48.89% to 58.98% and 76.80% to 80.15% at a constant mass flow rate 0.0083kg/s and 0.083kg/s respectively. The results found that for fin height 2.8cm and fin spacing 1cm, the effective efficiency increases from 58.98% to optimal value 74.91% with increase in mass flow rate 0.0083-0.0416kg/s, subsequently decreases with further increases in mass flow rate. Results also show that for fin spacing 2.5cm and 5cm the optimal value is 76.36% and 75.92% at mass flow rate 0.066kg/s and 0.083kg/s respectively. Increasing mass flow rate as well as decreasing fin spacing cause increase pressure drop and friction factor, hence the difference between the thermal efficiency and effective efficiency increases remarkably and after optimal value the effective efficiency decreases with increase in mass flow rate or even effective efficiency decreases below the plane solar air heater. Increase in the fin height from 1.8cm to 4.8cm results in thermal efficiency decrease from 80.4% to 77%. This causes decrease in the surface conductance of fins. For constant fin spacing and fin height 1.8cm, the effective efficiency increases from 58.25 to maximum value 72.84 for mass flow rate 0.0083kg/s to 0.0416kg/s and then after decreases up to 52.24% with further increase in mass flow rate. This is attribute to increases the pressure drop in the louvered channel. The result revealed that fin spacing w=1cm and fin height 1.8cm and 3.8cm, the increasing solar intensity leads to increase in temperature rise linearly while the solar intensity has little effect on thermal efficiency for a given mass flow rate.

REFERENCES

[1] Yeh HM, Ho CD. (2009). Effect of external recycle on the performances of flat-plate solar air heaters with internal fins attached. Renewable Energy 34(5): 1340-1347. https://doi:10.1016/j.renene.2008.09.005

[2] Yeh HM. (2012). Upward-type flat-plate solar air heaters attached with fins and operated by an internal recycling for improved performance. Journal of the Taiwan Institute of Chemical Engineers 43(2): 235-240. https://doi.org/10.1016/j.jtice.2011.10.008

[3] Karim MA, Hawlader MNA. (2006). Performance investigation of flat plate, v-corrugated and finned air collectors. Energy 31(4): 452-470. https://doi.org/10.1016/j.energy.2005.03.007

[4] Handoyo EA, Ichsani D. (2016). Numerical studies on the effect of delta-shaped obstacles' spacing on the heat transfer and pressure drop in v-corrugated channel of solar air heater. Solar Energy 131: 47-60. http://dx.doi.org/10.1016/j.solener.2016.02.031

[5] Chabane F, Moummi N, Benramache S. (2014). Experimental study of heat transfer and thermal performance with longitudinal fins of solar air heater. Journal of Advanced Research, 5(2): 183-192. http://dx.doi.org/10.1016/j.jare.2013.03.001

[6] Sabzpooshani M, Mohammadi K, Khorasanizadeh H. (2014). Exergetic performance evaluation of a single pass baffled solar air heater. Energy 64: 697-706. http://dx.doi.org/10.1016/j.energy.2013.11.046

[7] Priyam A, Chand P. (2016). Thermal and thermohydraulic performance of wavy finned absorber solar air heater. Solar Energy 130: 250-259. http://dx.doi.org/10.1016/j.solener.2016.02.030

[8] Ho CD, Chang H, Wang RC, Lin CS. (2013). Analytical and experimental study of recycling baffled double-pass solar air heaters with attached fins. Energies 6(4): 1821-1842. http://dx.doi.org/10.3390/en6041821

[9] Maheshwari BK, Karwa R, Gharai SK. (2011). Performance study of solar air heater having absorber plate with half-perforated baffles. ISRN Renewable Energy 2011. http://dx.doi.org/10.5402/2011/634025

[10] Webb RL, Trauger P. (1991). How structure in the louvered fin heat exchanger geometry. Experimental Thermal and Fluid Science 4(2): 205-217. https://doi.org/10.1016/0894-1777(91)90065-Y

[11] Sahnoun A, Webb RL. (1992). Prediction of heat transfer and friction for the louver fin geometry. Journal of Heat Transfer 114(4): 893-900. http://dx.doi.org/10.1115/1.2911898

[12] Turizo-Santos J, Barros-Ballesteros O, Fontalvo-Lascano A, Vasquez-Padilla R, Bula-Silvera A. (2015). Experimental characterization of thermal hydraulic performance of louvered brazed plate fin heat exchangers. Revista Facultad de Ingeniería Universidad de Antioquia (74): 108-116.

[13] Vorayos N, Kiatsiriroat T. (2010). Thermal characteristics of louvered fins with a low-reynolds number flow. Journal of Mechanical Science and

Technology 24(4): 845-850. http://dx.doi.org/10.1007/s12206-010-0310-y
[14] Achaichia A, Cowell TA. (1988). Heat transfer and pressure drop characteristics of flat tube and louvered plate fin surfaces. Experimental Thermal and Fluid Science. https://doi.org/10.1016/0894-1777(88)90032-5
[15] Chang YJ, Wang CC. (1997). A generalized heat transfer correlation for Iouver fin geometry. International Journal of Heat and Mass Transfer. https://doi.org/10.1016/0017-9310(96)00116-0
[16] Shah RK and Sakulic DP. (2003). Surface Basic Heat Transfer and Flow Friction Characteristics. Fundamentals of heat exchanger design. John Wiley & Sons.
[17] Kraus AD, Aziz A, Welty J. (2002). Compact Heat Exchangers. Extended surface heat transfer. John Wiley & Sons.
[18] Duffie JA, Beckman WA. (2013). Flat Plate Collector. Solar engineering of thermal processes. John Wiley & Sons.
[19] Watmuff J H, Charters WWS, Proctor D. (1977). Solar and wind induced external coefficients-solar collectors. Cooperation Mediterraneenne pour l'Energie Solaire, 56.
[20] Heaton HS, Reynolds WC, Kays WM. (1964). Heat transfer in annular passages. Simultaneous development of velocity and temperature fields in laminar flow. International Journal of Heat and Mass Transfer 7(7): 763-781. https://doi.org/10.1016/0017-9310(64)90006-7
[21] Kays WM. (2012). Convective heat and mass transfer. Tata McGraw-Hill Education.
[22] Dong J, Chen J, Chen Z, Zhang W, Zhou Y. (2007). Heat transfer and pressure drop correlations for the multi-louvered fin compact heat exchangers. Energy Conversion and Management 48(5): 1506-1515. https://doi.org/10.1016/j.enconman.2006.11.023
[23] Karwa R, Chitoshiya G. (2013). Performance study of solar air heater having v-down discrete ribs on absorber plate. Energy 55: 939-955. https://doi.org/10.1016/j.energy.2013.03.068

NOMENCLATURES

A	Area: A_p (absorber plate), A_c (Collector), m^2
C_p	Specific heat of air, J/kgK
C_f	Conversion factor
D_h	Hydraulic diameter, m
f	fanning friction factor
F	Collector efficiency factor
F_r	Heat removal factor
Fe_L	Flow efficiency for Re_L
Fe	Flow efficiency
H	duct height, m
H_f	fins height, m
h_r	Radiative heat transfer coefficient: $h_{r,1c}$ (absorber plate and glass cover), $h_{r,ca}$ (glass cover and ambient), $h_{r,12}$ (absorber plate and bottom plate), W/m^2K
h_c	Convective heat transfer: $h_{c,1f}$ (absorber plate and air stream), $h_{c,f2}$ (bottom plate and air stream), W/m^2K
I	Insolation, W/m^2
j	Colburn factor
K_f	Thermal conductivity of fins, W/mK
k	Thermal conductivity of air,W/mk
L_1	Length of solar collector, m
L_2	Width of solar collector, m
l_p	Louvered Pitch, m
l_l	Louvered length, m
$\dot{m}$	Mass flow rate, kg/s
n	Number of fins
P_{mech}	Mechanical power (W)
Q_u	Useful heat gain, W
Re_L	Reynolds number based on louver
Re_{lp}	Reynolds number between the louver pitch
Re	Reynolds number
T_a	Ambient temperature K
T_i	Inlet fluid temperature (K)
T	Mean temperature: T_c (glass cover), T_2 (bottom plate), T_f (fluid), T_1 (absorber plate), K
t	Fin thickness (m)
U_b	Bottom loss coefficient (W/m^2K)
U_L	Top loss coefficient (W/m^2K)
V_w	wind velocity (m/s)
V_{acc}	Accelerated air flow (m/s)
V_l	Flow velocity over the louver(m/s)
V	Fluid velocity (m/s)
Q_u	Useful heat gain (W)

Greek symbols

α	Absorptivity: α_c (glass cover), α_1 (absorber plate)
ε	Emissivity: ε_1 (absorber plate), ε_2 (bottom plate), ε_c (glass cover)
τ_c	Transmissivity of glass cover
η	Thermal efficiency
η_{eff}	Effective efficiency
η_f	Fin efficiency
ρ	Density of air (kg/m^3)
σ	Stefan's constant ($5.67x10^{-8}Wm^2 K^{-4}$)
Δp	Pressure drop (N/m^2)
θ_l	Louvered angle (^{o})